Analysis of Crack Propagation Rate in Steel Pipeline

Prince O. Agbainor[1] and S. Odi-Owei[2]
[1]*Department of Mechanical Engineering, Faculty of Engineering, University of Port Harcourt, P.M.B. 5323, Choba, Port Harcourt, Nigeria.*

[2]*Department of Mechanical Engineering, Faculty of Engineering, Rivers State University of Science and Technology, Port Harcourt, Nigeria.*

Abstract

For the stability assessment in piping components, it is important to determine the point of initiation of a crack, and to monitor and diagnose the subsequent crack propagation behavior as well as the failure patterns, to ensure pipeline structural integrity. This research analytically determines the crack propagation rate by the use of Improved crack tip opening area, (CTOA), and limiting crack speed,(LCS), models and subsequently predict the crack propagation behavior under fatigue loading. With reference to steel pipelines, inspection of sample data from Murtagian's work is simulated and compared with analytically developed model and the results compared and eventually used to determine the depth of crack. Levenberg-Marquardt Algorithm, (LVA), was developed as an optimization tool to determine crack growth evolution. Also, the probability of pipeline failure caused by crack growth and uncertainties related to loads and material properties of the structure is estimated using a new Monte Carlo simulation technique.

Keywords*: Crack Driving Force, Crack length, Limiting Crack speed, Crack tip opening area, Dynamic material toughness.*

1. Introduction

Oil and Gas transmission pipelines usually have a good safety record. This is due to a combination of good design, materials and operating practices. However, like any engineering structure, pipelines do occasionally fail, and such failures do have economic implications and are sometimes catastrophic, leading to loss of human life. The performance of an engineered system or product is often affected by unavoidable uncertainties [1]. The most common causes of damage and failures in onshore and offshore oil and gas transmission pipelines are external interference (also known as mechanical failure), corrosion and sabotage. Cracks occurring during the fabrication of a pipeline are usually assessed against recognized and proven control limits. Pipeline failures are often related to a breakdown in a system such as the corrosion protection system has become faulty and a combination of ageing coating, aggressive environment and rapid corrosion growth may lead to corrosion induced failure.

Fatigue plays a very important role in piping systems and may lead to crack initiation from either the highly stressed regions or the flaws. The crack initiation and subsequent propagation may be avoided in any piping system. These pipe installations occasionally experience high amplitude vibration (e.g. seismic vibration) which may initiate/extend the existing cracks [10]. The monitoring of the cracks becomes more significant in the installation of a pipe carrying hazardous fluid. The design for through-wall-cracked pipe (TWC) is leak-before-break (LBB), based on fracture mechanisms concepts have also been adopted for fail-safe design criteria.

The LBB demonstration which is based on failure mechanisms requires information on the initial size of a defect, initiation of crack growth from the inherent defect and subsequent crack growth rates. The nature of crack will grow and penetrate the wall thickness under fatigue loading. Thereafter, the crack will grow in a circumferential direction under cyclic loading.

Generally, fatigue crack growth depends on the initial crack length, materials properties, dimensions and loading conditions, etc.

In the past, analyzing the theoretical and technological aspects of pipeline bursting tests in which fracture propagation and arrest behavior were determined through measurement of fracture extension vs. time, depressurization, and strain at several points were expensive and time consuming, but they rendered useful and instrumental information on pipeline behavior. The battelle-curves semi-empirical analysis was one of the first methods used by the industry to predict the arrest of dynamic ductile propagating fractures. The method is based on the correlations of full scale testing with results of the CVN (Charpy Vee Notch) test [6]. More recently, a method based on the CTOA (crack tip opening angle) was proposed for characterizing the toughness of steel pipelines by the use of two-specimen CTOA test [5]. These specimens are three-point bend specimens similar to the drop-weight tear test (DWTT) specimen, and the methods based on dynamic fractures [8] which are relatively simple and inexpensive, give partial information on actual pipeline behaviour, and in many cases do not allow a proper assessment of it.

Shashi [10] proposed the gamma model (γ-model) to account for a tremendous amount of uncertainty and difficulty in predicting and measuring the crack growth. The gamma model was used to determine the next depth of crack by introducing a non-dimensional number and crack fitting or varying the exponent values. The γ-model was also applied on single edge notch tension (SENT) specimen.

Within the last three decades, several other models for the analysis of crack propagation were also developed, since the determination of the crack initiation. The research work by Murtagian and others [7] proposed the CTOA (crack tip opening angle) for characterizing the toughness of steel pipeline by the use of the two-specimen CTOA test [8]. They used three-point bend specimens, and the method requires a minimum CTOA for a given material to prevent crack propagation.
Murtagian and others [7] failed to consider non-classical tools in their approach. Thus, the work seeks to address the knowledge gap in Murtagian's investigation. A non-classical approach is adopted in this work.

2. Materials and Methods

The proposed use of the material dynamic toughness on the governing equation of the crack motion accounts for the combination of effects of the finite rate of energy transfer by the elastic waves and the static material toughness. Inertia effects are considered by computing the momentum of the effective mass that is moving at the crack speed. This mass acts as an additional material resistance to crack growth when the crack is accelerating, and as an additional crack driving force when the crack is decelerating, extending the crack beyond the point that would be expected in a static analysis. The schemes employed are shown diagrammatically in figures 1 and 2.

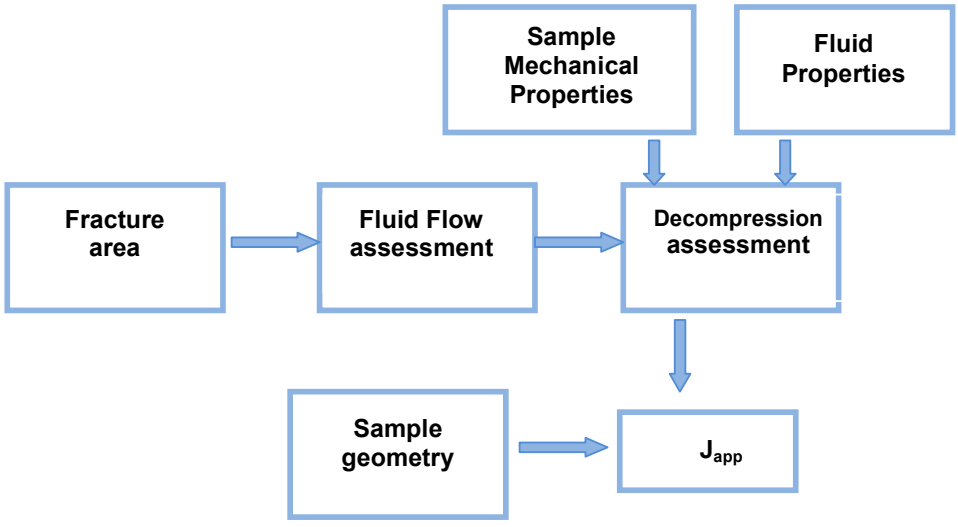

Figure 1. Input/output scheme for crack driving force estimation

Fig 2 below shows the process, variable dependence and the loop scheme adopted for the numerical solution.

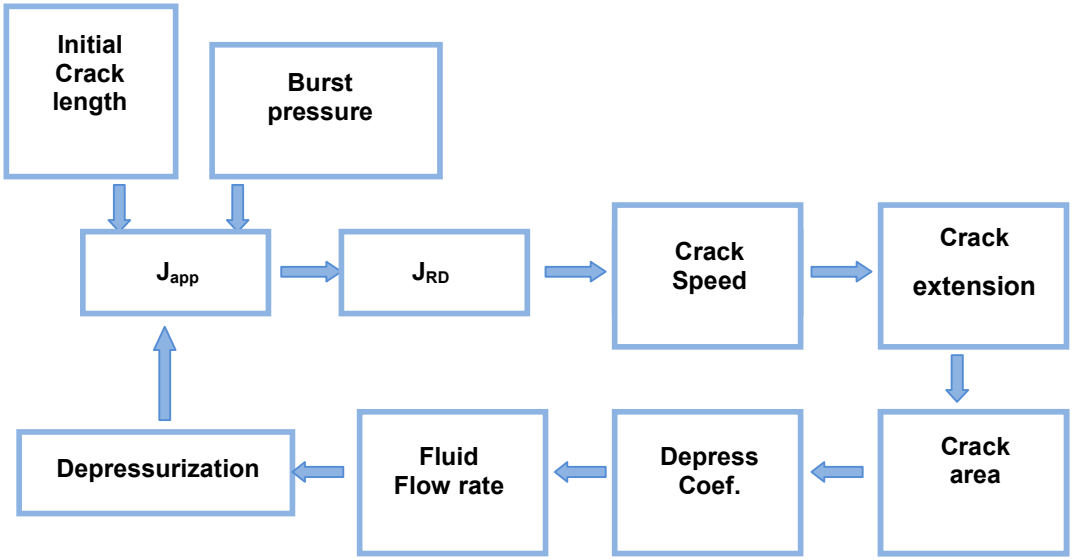

Figure 2. Numerical loop scheme for solving crack growth problem

The model here developed is based in the momentum conservation principle shown in Eq. (2.1)

$$d(m.v) = F.dt \qquad (2.1)$$

where v is the crack speed, m the mass in motion, F the motion driving force, and t time. As a function of crack length this equation becomes

$$\frac{dm}{da}.v^2 + m.v.\frac{dv}{da} = F \qquad (2.2)$$

It is postulated that the motion driving force is given by the difference between the crack driving force (J_{app}) and the dynamic material toughness (J_{RD}) as shown in Eq. (2.3)

$$F = J_{app} - J_{RD} \qquad (2.3)$$

By physical constraints, v cannot exceed v_{LIM}. Therefore for a steady state crack propagation, when

$v \rightarrow v_{LIM}$ Eq. (2.2) becomes Eq. (2.4)

$$\frac{dm}{da}.v_{LIm}^2 = J_{app} - J_{RD} \qquad (2.4)$$

From Eq. (2.4), the (variable) effective specimen mass as shown in Eq. (2.5), can be defined. It is assumed that this effective mass is located at the crack tip [9]

$$m = \frac{1}{v_{LIm}^2}.\left(\int_0^a Japp - \int_{a_0}^{a} J_{RD}\right)da \qquad (2.5)$$

Note that in Eq. (2.5) the lower limit of integration varies for J_{app} and J_{RD}. For J_{app} this limit is zero, i.e. the process starts at a = 0, while for J_{RD} it is the initial crack length. An effective initial mass m_0 can be obtained for the onset of crack propagation as

$$m_0 = \frac{1}{v_{Lim}^2}.\int_0^{a_0} J_{app}\,da \qquad (2.6)$$

Replacing Eqs. (2.3) – (2.5) into Eq. (2.2) the differential equation of the dynamic crack propagation is obtained as shown in Eq. (2.9)

$$\left(\frac{v}{v_{Lim}}\right)^2 + \frac{v}{v_{app}^2}.\frac{\int\left(J_{app} - J_{RD}\right)da}{\left(J_{app} - J_{RD}\right)}.\frac{dv}{da} - 1 = 0 \qquad (2.7)$$

By solving Eq. (2.7) it is possible to find the instantaneous values of the crack tip position and its velocity. It should be noted that J_{app}, J_{RD} and v are unknowns and strongly coupled. For the limit case when $v \rightarrow v_{LIM}$, it can be seen that $dv/da \rightarrow 0$.

2.1. Crack driving force J_{app}

To obtain the exact analytical solution for the crack driving force, spatial fluid pressure evolution, body inertial forces, specimen geometry changes and stress wave reflections must be considered [5]. A simplified analysis was used here to compute the crack driving force based on the works of Erdogan and Kilber [2] and Folias [3], for a pressurized cylinder with an axial through-the-wall crack including the crack tip plasticity and geometry corrections to the plate solution. Considering the relation shown in Eq. (2.8) the solution for the crack driving force when plasticity is present is given by Eq. (2.9)

$$J_{app} = \frac{K_{app}^2}{E} \qquad (2.8)$$

Where E is the Elastic modulus of the material

$$J_{app} = \frac{\sigma_h^2 \cdot \pi \cdot a}{E} \cdot \left[1 + \left(\frac{\sigma_h}{\sigma_0}\right)^2\right] \cdot \left(1 + 1.25\lambda^2\right)$$

$0 < \lambda \leq 1$ (2.9a)

$$J_{app} = \frac{\sigma_h^2 \cdot \pi \cdot a}{E} \cdot \left[1 + \left(\frac{\sigma_h}{\sigma_0}\right)^2\right] \cdot \left(0.6 + 0.9\lambda\right)^2 \quad 1 < \lambda \leq 5 \quad (2.9b)$$

Where

$$\lambda = \frac{a}{\sqrt{R \cdot t_h}} \qquad (2.10)$$

The hoop stress in Eq. (2.9) is dependent on the variable fluid pressure on the sample. In this problem the crack length and the applied load are coupled variables; the scheme to compute the crack driving force is shown in figure 2 above. Fracture area (A), fluid and sample mechanical properties are necessary inputs for the computation of the crack driving force. The fracture area evolution is assumed to grow proportionally to the crack length. The initial and final crack lengths are obtained analytically.

Conservation of mass and energy was utilized for the calculation of depressurization. The total fluid mass that can flow through the crack area is given by:

- elastic volumetric sample deformation, and
- the change of specific volume of the fluid inside the sample as shown in Eq. (2.12)

$$\frac{dm}{dp} = \frac{\partial v}{\partial p} \cdot \rho + v \cdot \frac{\partial \rho}{\partial p} \qquad (2.11)$$

In Eq. (2.11) the term $\frac{\partial v}{\partial p}$ is the specimen mechanical volume variation and $\frac{\partial \rho}{\partial p}$ is the fluid compressibility (ξ), V being the sample internal volume, and ρ the fluid density. For a cylindrical specimen of length L

$$\frac{\partial V_{(R,L)}}{\partial p} = 2 \cdot \pi \cdot R \cdot L \cdot R^2 \cdot \frac{\partial R}{\partial P} + \pi \cdot R^2 \cdot \frac{\partial L}{\partial P} \qquad (2.12)$$

from linear elasticity

$$\frac{\partial R}{\partial P} = \frac{R^2}{E \cdot t_h} \cdot \left(1 - \frac{v}{2}\right) \qquad (2.13)$$

And

$$\frac{\partial L}{\partial P} = \frac{R}{E \cdot t_h} \cdot L \cdot \left(\frac{1}{2} - v\right) \qquad (2.14)$$

For steels $v \approx 0.3$, then $[(2 - v) + (1 - 2.v)] \approx 2$, giving

$$\frac{\partial V_{(R,L)}}{\partial p} = \frac{2 \cdot \pi \cdot R^3 \cdot L}{E \cdot t_h} \qquad (2.15)$$

To simplify the problem, it is assumed that the there is no pressure gradient in the sample and that the fluid flow, and consequently the depressurization, is dependent on a depressurization coefficient (ψ) function of the crack speed with the form expressed in Eq. (2.17). If $v \geq v_{fw}$ it is assumed that no depressurization takes place,

$$\left.\begin{array}{l} \psi = 1 - \frac{v}{v_{fw}}; \ 0 < v \leq v_{fw} \\ \psi = 0; \ v < v_{fw} \end{array}\right\} \qquad (2.16)$$

The mass fluid flow (Q_m) is given by Eq. (2.17)

$$Q_m = \frac{dm}{dt} = \Psi \cdot \eta \cdot \rho \cdot A \cdot v_{fl} \qquad (2.17)$$

Where η is the system hydraulic discharge coefficient, assumed to be of unitary value for all the experiments, A is the crack opening area, and v_{fl} the fluid flow velocity through the fracture area, which can be computed using Bernoulli's theorem, p being the hydrostatic pressure and ρ the fluid density inside the specimen.

$$v_{fl} = \sqrt{\frac{2.p}{\rho}} \qquad (2.18)$$

Using Eqs. (2.11), (2.15), (2.17) and (2.18), disregarding the variations of R, ρ, and V with pressure by using their initial values, and making two variable substitutions, it can be deduced that the hoop stress drop by crack extension can be expressed as

$$\frac{d\sigma_h}{da} = \frac{\sqrt{\sigma_h}}{v} \cdot A \cdot \psi \cdot \frac{\eta \cdot \sqrt{\frac{R}{t_h}} \cdot \sqrt{\frac{2}{\rho}}}{V \cdot \left[\frac{2 \cdot R}{E \cdot t_h} + \rho \cdot \xi\right]} \qquad 2.19$$

Eq. (2.19) has four strongly coupled variables: hoop stress, crack speed, crack opening area, and depressurization coefficient. The remaining terms of the equation are constant for a given test. A typical parameterized decompression curve can be seen in Figure 3 below.

To find the crack length evolution, the differential system of Eqs. (2.7) and (2.19) has to be solved. Hence, a Matlab program was developed to accomplish this task.

Table 1. Specimen Geometry/Material Properties

Radius	T_h (mm)	Length (m)	Hoop Tension (MPa)	Hoop Stress (MPa)
50	10	2	1500	1200
50	10	2	1500	1200

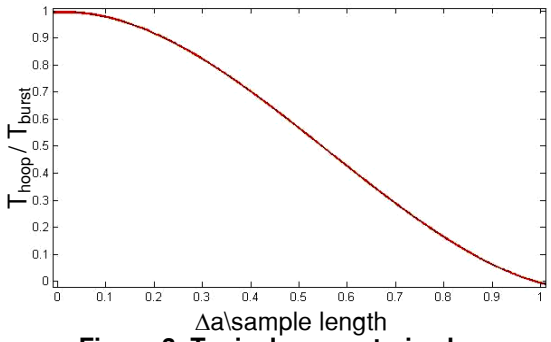

Figure 3. Typical parameterized decompression curve

2.2. Dynamic material toughness (J_{RD})

By extending the work of Kanazawa and others [4] to the case of elastoplastic dynamic fracture, the functionality shown in Eq. (2.20) is proposed for the material dynamic toughness

$$J_{RD} = \frac{J_{R(\Delta a)}}{\left(1 - \frac{v}{v_{Lim}}\right)^{M}} \qquad (2.20)$$

The exponent M is considered to have a value of 0.5, v_{LIM} is a temperature dependent parameter obtained empirically, and $J_R(\Delta a)$ is the material resistance curve obtained from static fracture tests, which can also be expressed as Eq. (2.21). The material parameters J_{IC}, α, and n, are obtained by testing.

$$J_{R(\Delta a)} = J_{IC} + \alpha \cdot (\Delta a)^{n} \qquad (2.21)$$

To validate the effectiveness of the model, the optimal values of the test variables are compared with the existing models of Murtagian and others [7]. The overall numerical results are thus summarized.

2.3. New Model based on Levenberg-Marquart Algorithm

From Eq. (2.19), we develop a function which will be use to fit set of data to obtain optimum solution for our crack model.

$$\text{If } \frac{d\sigma_h}{\sqrt{\sigma_h}} = \frac{T_{hoop}}{T_{burst}} = dt_{hb} \qquad (2.22)$$

$$\text{And } k = \frac{\eta \cdot \sqrt{\frac{R}{t_h}} \cdot \sqrt{\frac{2}{\rho}}}{V \cdot \left[\frac{2 \cdot R}{E \cdot t_h} + \rho \cdot \xi\right]} \qquad (2.23)$$

$$\text{Then, } \frac{dt_{hb}}{da} = \frac{A}{v}.\psi.k \qquad (2.24)$$

But ψ is defined from Eq. (2.16) and we then obtain Eq. (2.25) as below;

$$\frac{dt_{hb}}{da} = \frac{A.\left(1 - \frac{v}{v_{fw}}\right).k}{v} \qquad (2.25)$$

If $v_{fw} = 1$ since $v_{\lim} < v_{fw}$, and since crack growth is on dependent on k we set the other parameter of k to unity, i.e $k = 1$, we now obtain the expression for the change in hoop and burst tension with respect to the crack extension as,

$$\frac{dt_{hb}}{da} = \frac{A.(1-v).k}{v}, \quad \frac{dt_{hb}}{da} = A.\left(\frac{1-v}{v}\right).k \qquad (2.26)$$

Taking an assumption based on inference for the crack speed with a range between 0 – 1500 [m/s] and scaling to between zero and one (for realistic uniform random distribution), we define v as 0.5[m/s], then if we plunge it into Eq. (2.26) with $k = 1$, we have;

$$\frac{dt_{hb}}{da} = A \qquad (2.27)$$

The changes for the hoop and burst tension with respect to the crack extension is obtain as the slope from the typical parameterized decompression curve in figure 3, where the coefficient of the curve using the curve fit tool (cftool) in MATLAB for the cubic is thus,

$$\frac{dt_{hb}}{da} = P_1 t^3 + P_2 t^2 + P_3 t + P_4 \qquad (2.28)$$

Dividing through by t we obtain Eq. (2.29) which is now equivalent to our crack growth area A. Therefore,

$$A = P_1 t^2 + P_2 t + P_3 + P_4 t^{-1} \qquad (2.29)$$

So A is the crack exponent growth function that that is used to fit the Levenberg-Marquart algorithm. The LM is to come up with the optimum coefficient of the given function that gives the least square error.

Table 2 and 3 below provides analytical tables for working;

Table 2. Specified Specimen Properties

J_{IC} (kJ/m^2)	A	N	v_{LIM} (m/s)
1000	250	0.5	1000
1100	250	0.5	6000
1200	250	0.5	8000
1300	250	0.5	3000
1400	250	0.5	2000
1500	250	0.5	1000

Table 3. Crack Area at Specified Conditions

tn	An
0	0
100	15.6798
200	15.6405
400	15.6210
600	15.6415
1000	15.6092

3. Results and Discussion

In this paper, a computer program was developed using the model developed, and a numerical simulation was carried out to determine the crack growth evolution in steel pipeline.

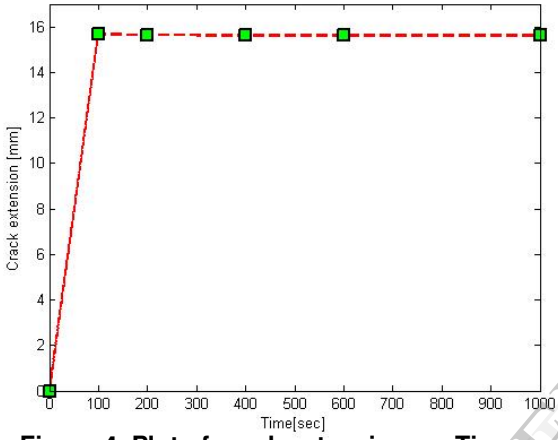

Figure 4. Plot of crack extension vs. Time

From the graph above, there was a gradual increase in the crack growth within the first 100 [secs], and thereafter the crack reaches it terminal where no further crack growth can occur (i.e. the limiting crack speed), where it maintain a linear growth after the first 100 [secs], the crack growth was now constant.

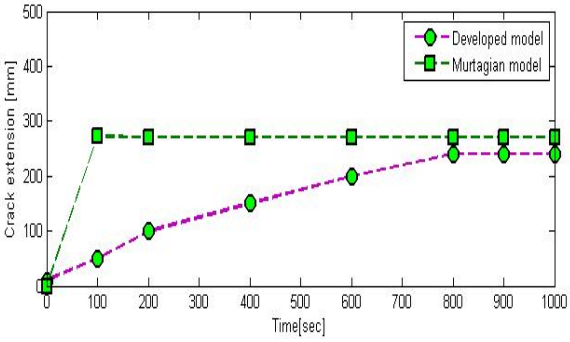

Figure 5. A plot showing the comparison be tween Murtagian□s and Developed model

From figure 5 above, it can be seen that unlike the Murtagian's model where the constant crack extension value of about 275 [mm] was attained rapidly within the first 100 [secs], the developed model displayed a uniform crack extension with respect to time(crack speed) before the constant crack extension was attained at 800 [sec]. So, the developed model could thus attain a constant crack extension rate at 275 [mm] progressively within 800 [sec]. The model showed a reasonable agreement in crack extension vs. time between Murtagian's and the developed model. It thus clearly deduced the model developed as a working model which can serve as a guide to the actual if operational data are used.

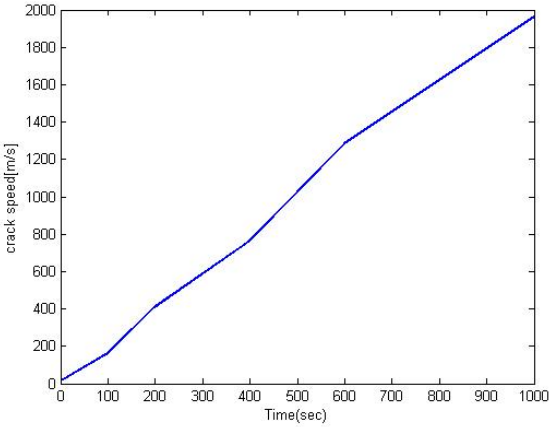

Figure 6. A graph of crack speed [m/s] vs. Time [sec]

From the graph, the acceleration tends to linearity after 600 [sec] at a speed range of approximately 1300 [m/s]. Thus, as an increase in time leads to a corresponding increase in the crack speed.

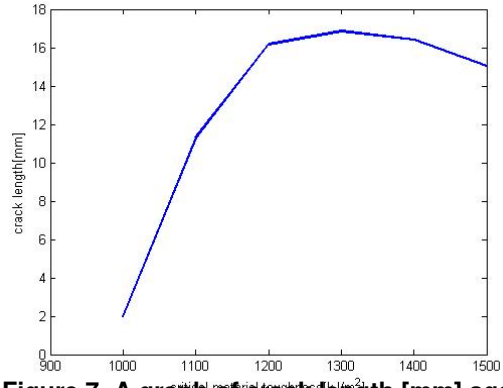

Figure 7. A graph of crack length [mm] agai nst critical material toughness [kJ/m^2]

The critical material toughness, between 1000 – 1100 [kJ/m^2] maintains linearity between 2 – 12 [mm] and thereafter form a linear curve as it increases and attains its peak at a crack length of 17 [mm]. Thus, the critical material toughness must have value over 990 [kJ/m^2] for prevention of crack propagation.

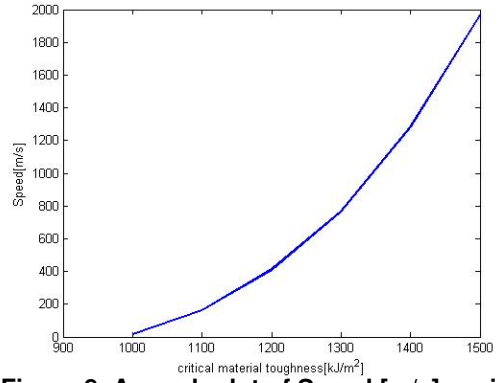

Figure 8. A graph plot of Speed [m/s] against critical material toughness [kJ/m^2]

The crack speed is observed to negligible for critical material toughness less than 1000 [kJ/m^2] but increases steadily for critical material toughness above 1000 [kJ/m^2].

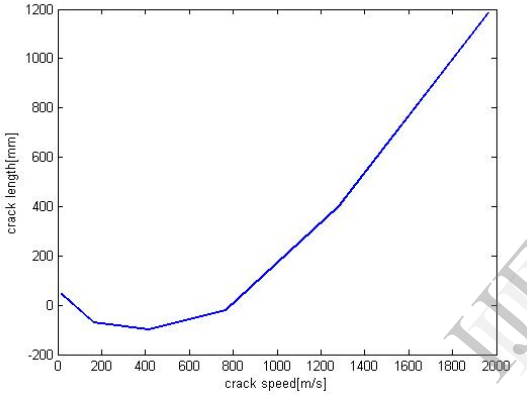

Figure 9. A graph plot of crack length [mm] against crack speed [m/s]

From figure 9 the minimum crack length was attain at the crack speed of 400 [m/s], and thereafter embarked on continuous in crack length as the crack speed increases.

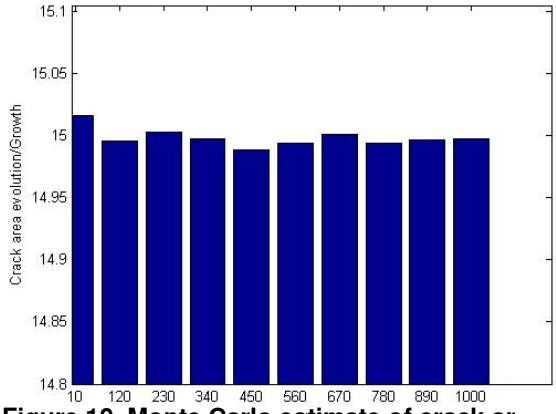

Figure 10. Monte Carlo estimate of crack area evolution

Hence after 1000 runs, the estimates for the crack growth produces good approximate to the mean from 160 values of the crack growth value for randperm (selecto-random permutation). Any optimize design will take the least size/memory with the least cost. Hence, Monte-Carlo optimized the best possible solution with the least possible data set.

Also, Monte-Carlo shows the possibility of reducing the amount of work by limiting the selection of points to regions where the sample mean (i.e. Crack growth values) was changing most rapidly.

Table 4 below shows the error that resulted after those numbers of simulations were carried out.

Table 4. Optimize values of Monte Carlo with error function

S/N	Runs	Mcarl	Error
1	10	15.01603	0.0232
2	120	14.99575	0.0029
3	230	15.00314	0.0103
4	340	14.99756	0.0047
5	450	14.98904	0.0038
6	560	14.99407	0.0012
7	670	15.00138	0.0086
8	780	14.9936	0.0008
9	890	14.99637	0.0035
10	1000	14.99777	0.005

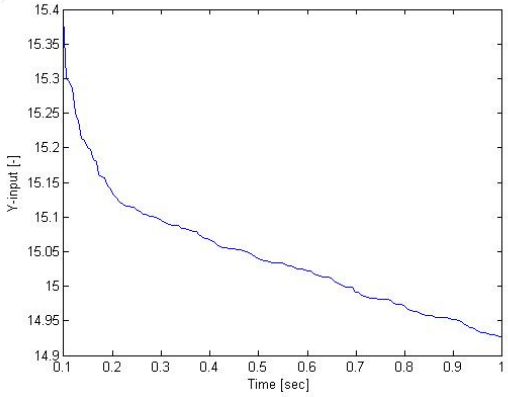

Figure 11. A plot of Y- input against time

Figure 11 shows the plot of the generated curve for crack growth for Levenberg-Marquardt algorithm with crack growth (A) as the initial guesses from developed model.

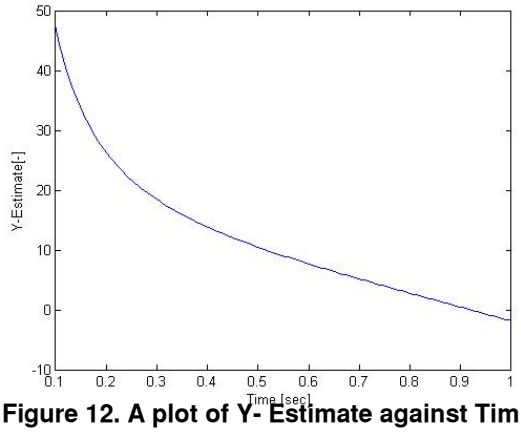

Figure 12. A plot of Y- Estimate against Time

The plot above shows the estimate value against time. At the stage the curves smoothened out.

The results for the various values of X1, X2, X3 and X4 for the given y-input values, that satisfies the non-linear least criteria as developed in the Matlab source code are provided below:

Table 5. Optimum values that satisfies the non-linear criteria for model parameters

X1	-5.4472
X2	-8.4472
X3	7.9528
X4	4.0528

The LM optimization thus showed the Levenberg-Marquardt algorithm as a good iterative procedure and illustrates the use of software to solve nonlinear least squares curve-fitting problem. The projected Levenberg-Marquardt method guarantee local fast convergence under suitable assumptions and shows that it is perfectly appropriate and good to use the best available estimate of the desired parameters as the initial guess, fitting the algorithm to converge to different local minima.

Fig 13 below shows the Simulink implementation of crack growth evolution. The limiting crack speed 'vss' and slope gain have been defined using constant Simulink blocks, while an embedded Matlab function block is used to compute the crack propagation area 'A' and a constant 'k' which defines crack growth over time. The crack growth model is controlled by using a multi port switch and a stopping criteria is enforced in the scaling subsystem [11].

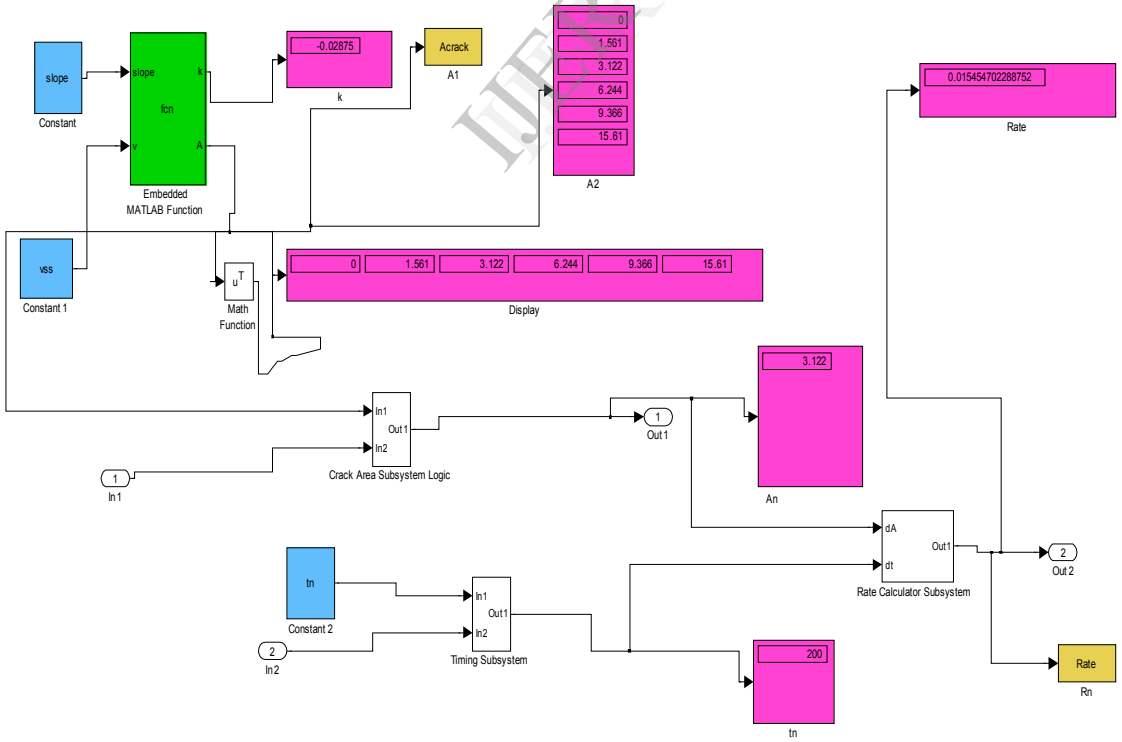

Figure 13. The model developed for crack growth evolution in Simulink

4. Conclusion

A software program is developed for the estimation of cracks based on crack tip opening area, CTOA and limiting crack speed, LCS models for steel cracked pipeline as a check of the experimental results of the samples considered. Thus, critical values for the test were generated using a Monte Carlo simulation procedure. To ensure pipe safety, such prediction becomes necessary for both simple and complex cracks in pipelines to determine the failure patterns for such pressure vessels. The model allows for quantitative prediction of crack length evolution with time.

With this approach, the effects of sudden failure associated with cracks in the pipe lines can be minimized.

The algorithm is needed to help site engineers solve relative problems of this nature.

5. References

[1] G. Apostolakis, The concept of probability in safety assessments of technological systems, Vol. 250, No. (4986): 1990, pp. 1359-64, Battelle Press, Columbus, OH.

[2] F. Erdogan and J.J Kibler, Cylindrical and spherical shells with cracks, Int J Fract Mech, vol (5), 1969, pp. 229-3.

[3] E.S. Folias, An axial crack in a pressured cylindrical shell. Int J Fract Mech, Vol (1), 1965, pp. 104 – 13.

[4] T. Kanazawa and S. Machida, "Fracture dynamics analysis on fast fracture and crack arrest experiments", In: Kanazawa T, Kobayashi AS, Lido K, editors. Fracture Tolerance Evaluation, Toyoprint, 1982.

[5] M.F, Kanninen, T.S Grant and G. Demofonti, "The development and validation of a theoretical ductile fracture model", In: Eighth symposium on line pipe research, paper 12, Arlington, VA: Pipeline Research Committee of AGA, 1993.

[6] W.A. Maxey, R.J. Eiber and R. J. Podlasek, "Observations on shear fracture propagation behavior", In: Symposium on crack propagation in pipelines, Institute of Gas Engineers, London, 1974.

[7] Murtagian and G. R. Ernst, D. H. Johnson and H. A. Ernst, Dynamic Crack Propagation In Steel line Pipe, Engineering Fracture Mechanics, 2005.

[8] D.L. Rudland, G. M. Wilkowski and Z. Feng, "Experimental investigation of CTOA in linepipe steels", 2003, pp. 567-77.

[9] D.K. Robert, A.A. Wells, The velocity of brittle fracture, Engineering 1954, 178:820-1.

[10] K. Shashi, "Prediction of Crack Propagation using gamma-model for through wall cracked pipes", Mechanical Engineering National Institute of Technology, Rourkela, 2011.

[11] N.E. Osegi, "An Introduction to mathematical modeling using simulink". 1st Ed. United State: Lulu publisher, 2011.